Met Office

Comparison of locally received MetOp-B IASI data with global MetOp-A IASI data

Forecasting Research Technical Report No: 575

19 February 2013

James Cameron

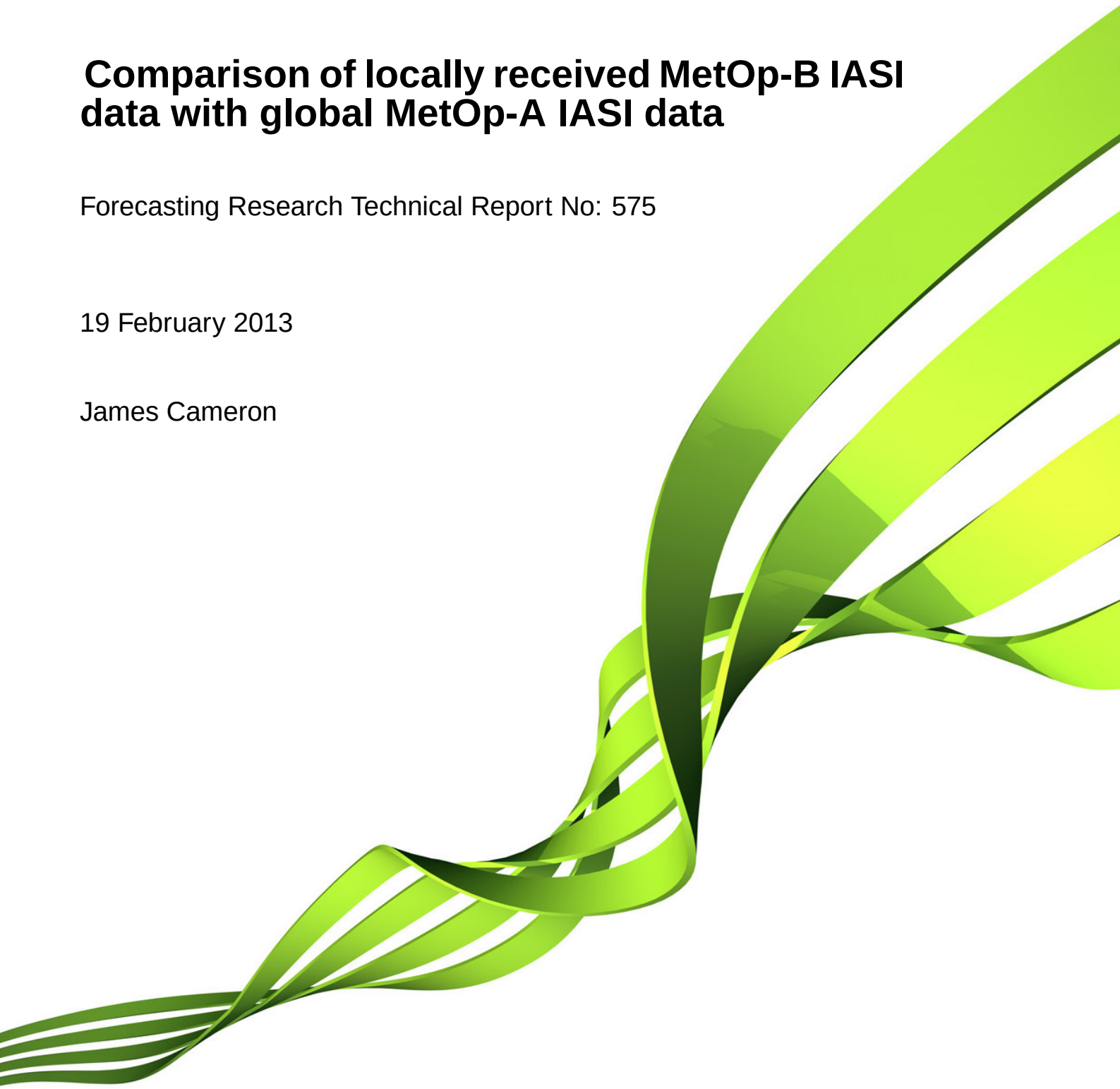

Abstract

Local MetOp-B IASI data has been received via direct broadcast at the Met Office and stored in an observation database since 21 November 2012. To assess the quality of this local data, the fit to forecast background was compared to the fit of MetOp-A observations for similar locations. The standard deviation of bias corrected minus forecast background is around 10% less for MetOp-B than for MetOp-A for the long-wavelength and short-wavelength channels, indicating a lower instrument noise in those channels. There is evidence that the spectral calibration of IASI MetOp-B data has been brought into closer agreement with IASI MetOp-A since 10 January 2013. IASI observations are made in groups of four. It is found that the bias of the four observations is very similar.

Contents

1 Introduction **3**

2 Comparison **3**

2.1 The data used in the comparison 3

2.2 Comparison with forecast background 6

2.3 Spectral calibration 15

2.4 Inter-pixel differences 15

3 Conclusions **19**

© Crown Copyright 2013

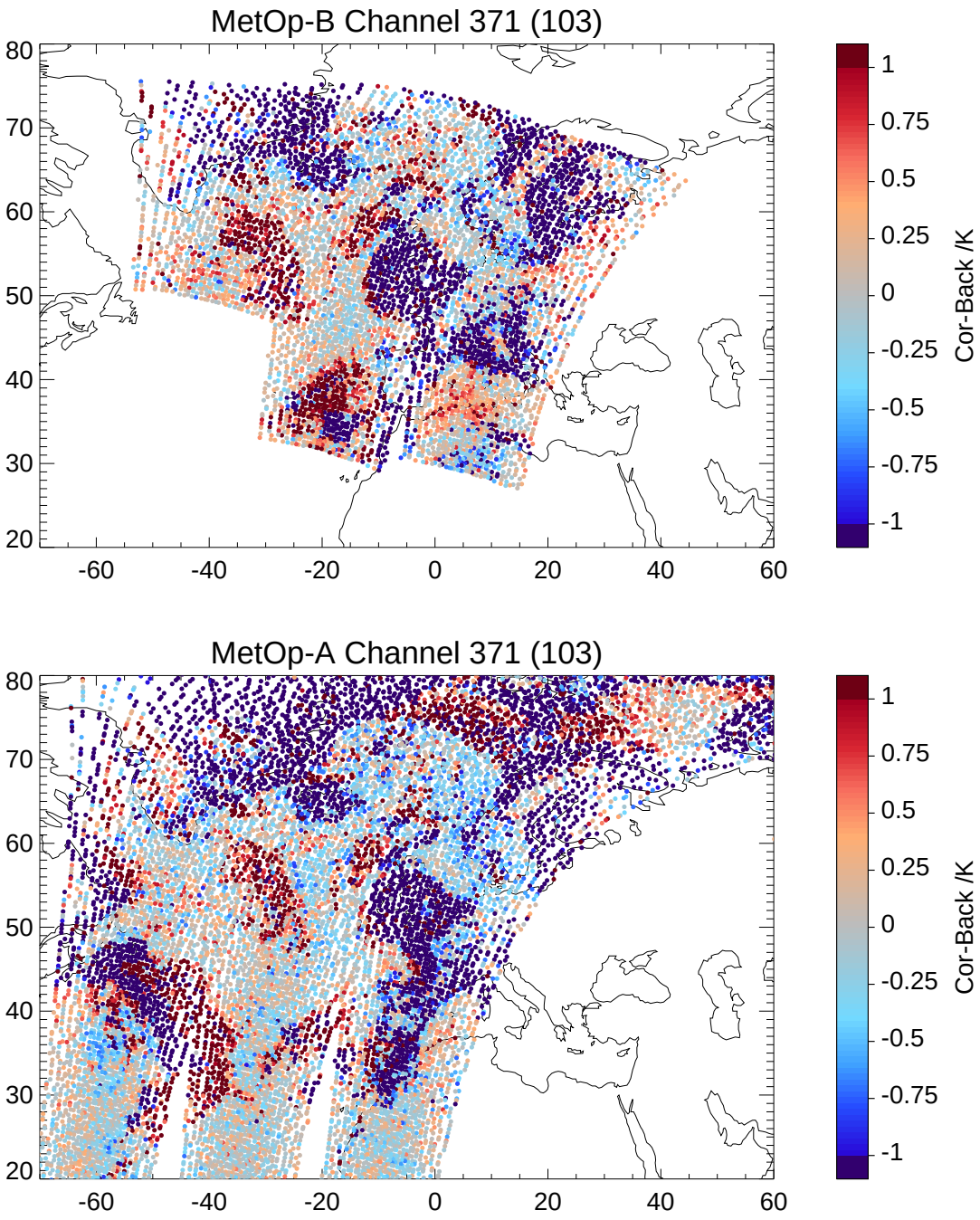

Figure 1: Locally received MetOp-B IASI data and global MetOp-A IASI data over Europe for the 12Z main run on 24 Nov 2012. The colours indicate the bias corrected minus forecast background brightness temperature for IASI channel 371 (MetDB channel 103, at 737.50 cm^{-1}).

© Crown Copyright 2013

1 Introduction

The EUMETSAT Polar System (EPS) MetOp mission consists of a series of three MetOp satellites. The first satellite, MetOp-A, was launched on 19 October 2006. MetOp-B was launched into a similar morning orbit on 17 September 2012. The two satellites are in the same orbital plane, 180° apart. To assess the quality of MetOp-B IASI data, the fit to forecast background is compared for MetOp-B and MetOp-A observations.

2 Comparison

2.1 The data used in the comparison

IASI data from MetOp-B has been received at the Met Office via direct broadcast and stored in the Met Office's observation database, the MetDB, since 21 November 2012. This data only covers areas the satellite is scanning while it is within range of the dish at Exeter. We receive MetOp-A IASI data both by direct broadcast and via EUMETCast. The data received via EUMETCast spans the entire globe and is referred to here as global data. Figure 1 shows locally received MetOp-B IASI data and global MetOp-A IASI data for 9–15Z 24 November 2012. Similar features can be seen, although it should be noted that neither the ground tracks nor overpass times exactly match.

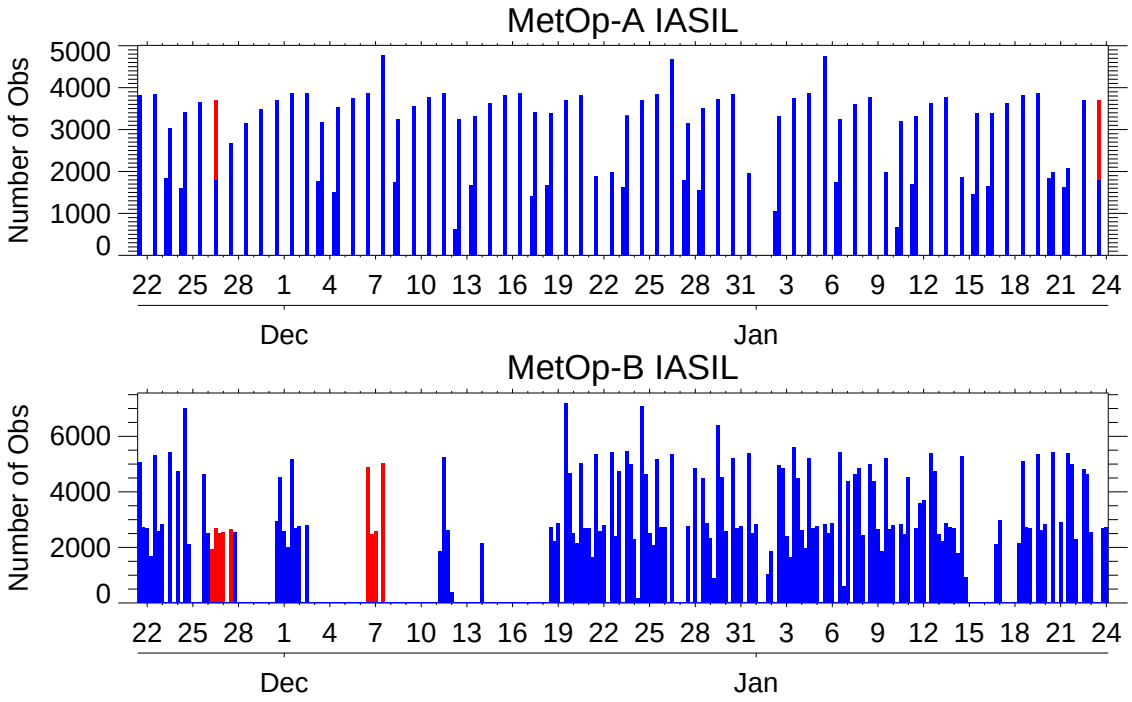

Figure 2: The number of locally received MetOp-A and MetOp-B IASI observations in each 6 hour data assimilation time window. Red bars indicate observations where the data quality flag is non-zero. Locally received MetOp-A data was not used in this study but is shown for comparison.

© Crown Copyright 2013

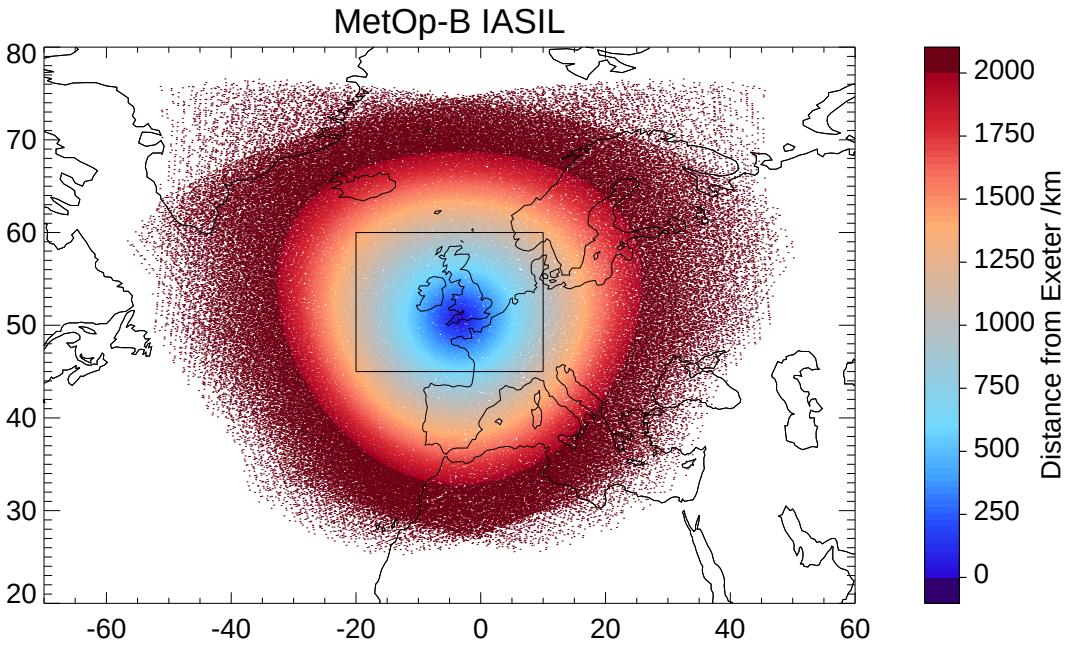

Figure 3: All locally received IASI MetOp-B observations from 18 Dec 2012–10 Jan 2013. Observations within 2000 km of Exeter were selected for study and are highlighted. The box shows the location of a sub-set of observations that were also studied

Figure 2 shows the number of locally received MetOp-A and MetOp-B observations present in the MetDB for each 6-hour data assimilation time window from 21 November 2012 to 24 January 2013. There is not as much locally received MetOp-A data as MetOp-B data because of the failure of the AHRPT transmitter on MetOp-A. MetOp-A data is only received locally for evening overpasses and even then the spatial coverage does not extend as far north.

In view of the missing MetOp-A local data, it was decided to compare locally received MetOp-B data to global MetOp-A data. To make the spatial sample as similar as possible, only observations within 2000 km of Exeter were included in the study. Figure 3 shows all MetOp-B observations received between 18 December 2012 and 10 January 2013. Observations within 2000 km of Exeter are highlighted. A sub-set of observations with longitude -20–10° East and latitude 45–60° North were used in the comparison and are shown in the figure. Figure 4 shows a histogram of the (approximate) density of MetOp-B observations versus distance. The observation density starts to drop after about 1000 km and turns down rapidly at about 2500 km. The observations from the MetOp-A global data set are assumed to be more evenly distributed. Figure 5 shows histograms of the time of day in UTC of all observations within 2000 km of Exeter from 18 December 2012 to 10 January 2013. Cloud free observations are shown as blue bars. Note that the distributions are similar but not identical.

All global MetOp-A and local MetOp-B IASI observations within 2000 km of Exeter were processed through the Met Office's observation processing system (OPS). The OPS is used for quality

© Crown Copyright 2013

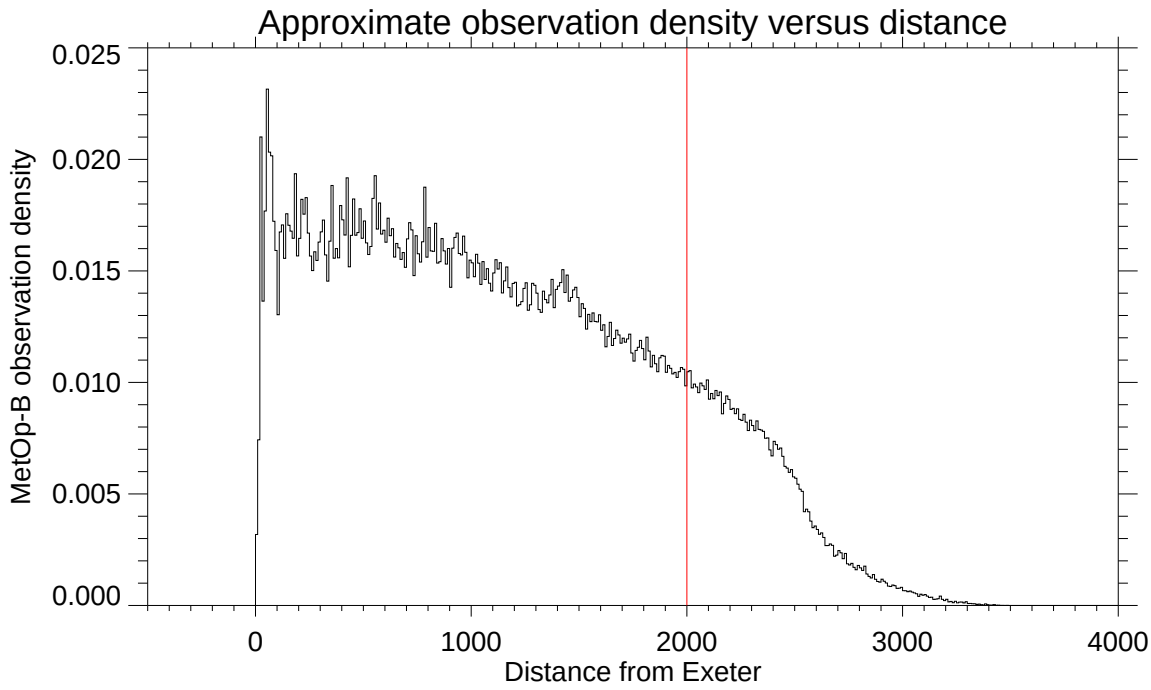

Figure 4: Histogram of the number of observations by distance, multiplied by the distance from Exeter in kilometres, divided by 2000, giving an approximate observation density.

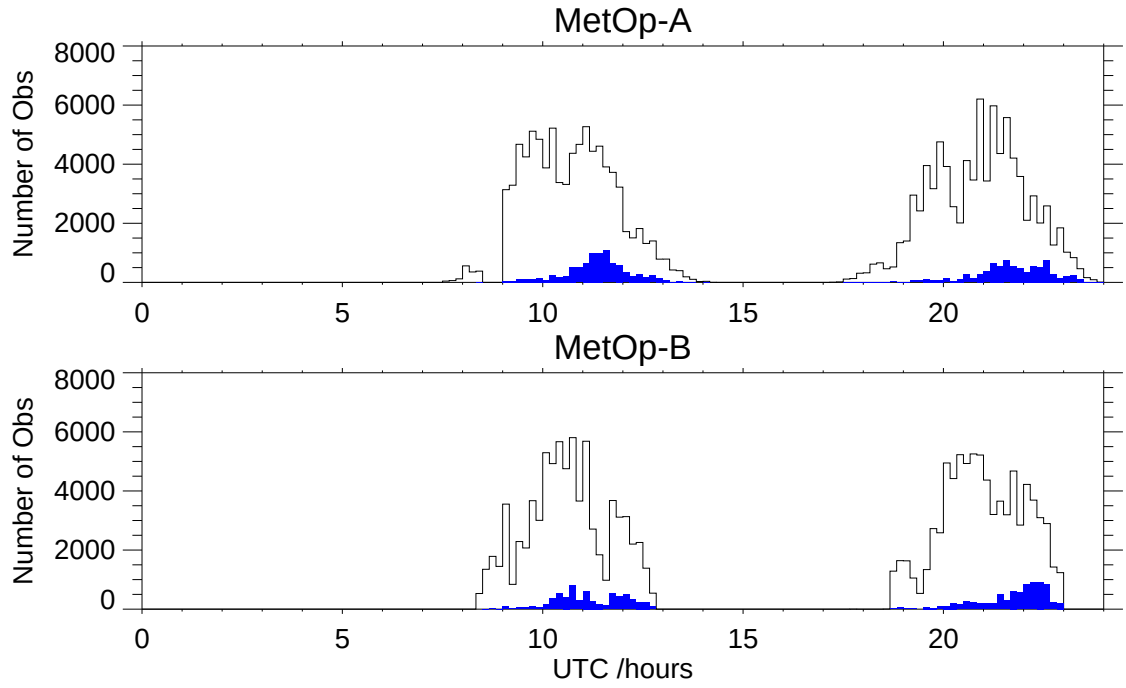

Figure 5: The time of day in UTC for all MetOp-A observations and all MetOp-B observations within 2000 km of Exeter between 18 Dec 2012–10 Jan 2013. Cloud-free observations (fitted cloud fraction $<$5%) are shown in blue.

© Crown Copyright 2013

control and to fit parameters to the observations that are not present in the 4D-Var control vector. Parameters fitted in the OPS are skin temperature, cloud top height, cloud fraction and, for observations over land, the surface emissivity. Only channels that peak well above the cloud top (where the integrated temperature Jacobian below the cloud top is less than 10% of the total integrated temperature Jacobian) or where the fitted cloud fraction is less than 5% are selected for assimilation. In this study the same bias correction, derived from December 2012 global MetOp-A data, was applied to both MetOp-A and MetOp-B data. Any 6-hour time window that did not include any MetOp-B observations were dropped from the study.

OPS statistics were gathered from three sets of observations:

Period 1 09Z 18 Dec – 03Z 10 Jan, within 2000 km of Exeter.

Box 1 09Z 18 Dec – 03Z 10 Jan, inside the latitude/longitude box shown in figure 3.

Period 2 21Z 10 Jan – 03Z 24 Jan, within 2000 km of Exeter.

The spectral calibration was updated on 10 January 2013, which is the reason the data is divided into periods 1 and 2. Most of the graphs in this report show statistics for all 314 IASI channels stored in the MetDB for cloud-free observations over the sea. Cloud-free is defined as having a fitted cloud fraction of less than 5%. In addition, only night-time observations contribute to the statistics for short-wavelength channels. A few of the graphs in this report show statistics for only those channels used in the 1D-Var retrieval and are either cloud-free or peak above the fitted cloud top – these channels are labelled as 'used channels' (this label is slightly misleading as a few of these channels are dropped before assimilation in VAR).

2.2 Comparison with forecast background

The upper plot of figure 6 shows the mean raw (un-bias-corrected) brightness temperature of MetOp-A (black) and MetOp-B (red) from the first time-period studied (Period 1) for cloud-free observations over the sea. Cloud-free observations were defined to be those with a fitted cloud fraction of less than 5%. The channels are plotted in the order in which they are stored in the MetDB. The long-wavelength channels are on the left and the short-wavelength ones on the right. The first 70 or so channels are stratospheric channels. Channels 70–125 are long-wavelength CO_2 temperature sounding channels. Next are some window channels, with the channels between 147 and 161 being strongly sensitive to ozone. The channels between about 170 and 270 are sensitive to water vapour and the remaining channels are short-wavelength.

The lower plot of figure 6 shows the difference in mean raw brightness temperature between MetOp-B and MetOp-A. The average brightness temperature is a little different across the board with the stratospheric channels being little colder in MetOp-B and most of the rest of the channels a bit warmer. These differences are probably because the spatial sampling and time-of-day distributions are not exactly matching for MetOp-B and MetOp-A. Figure 7 shows statistics for the same

© Crown Copyright 2013

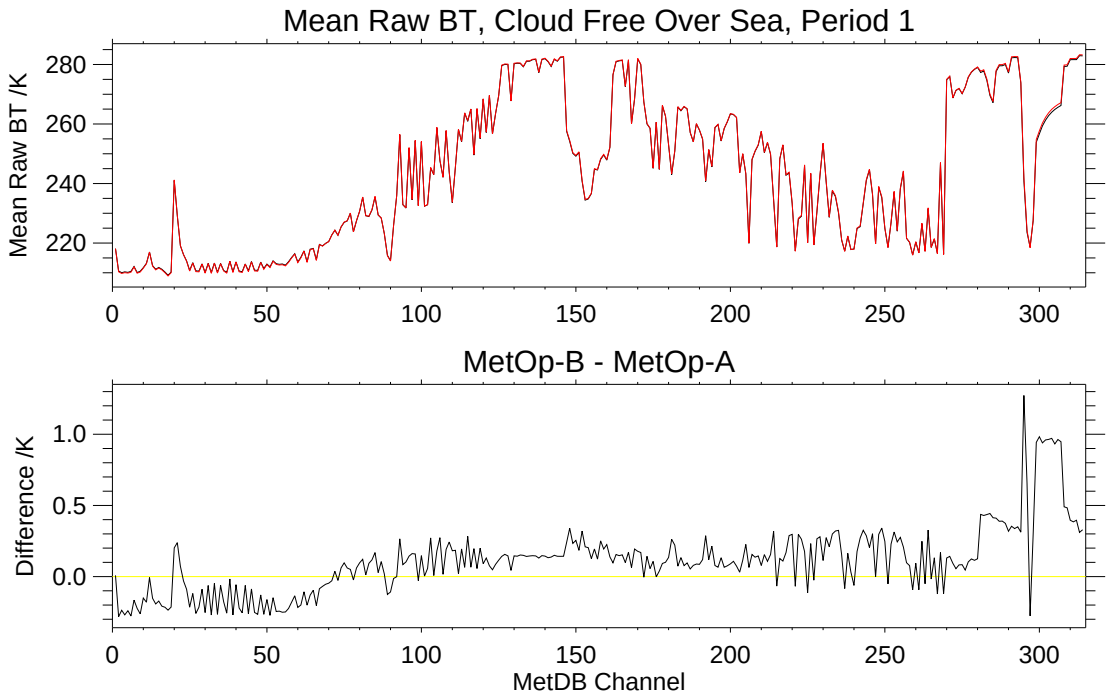

Figure 6: The upper plot shows the average raw brightness temperature of cloud-free observations over the sea from period 1 for IASI MetOp-A (black) and IASI MetOp-B (red). The red line for MetOp-B was plotted after the black line for MetOp-A and almost covers it. The lower plot shows the difference in average raw brightness temperature. The channels are shown in order of MetDB channel number, with the long-wavelength channels on the left and the short-wavelength ones on the right.

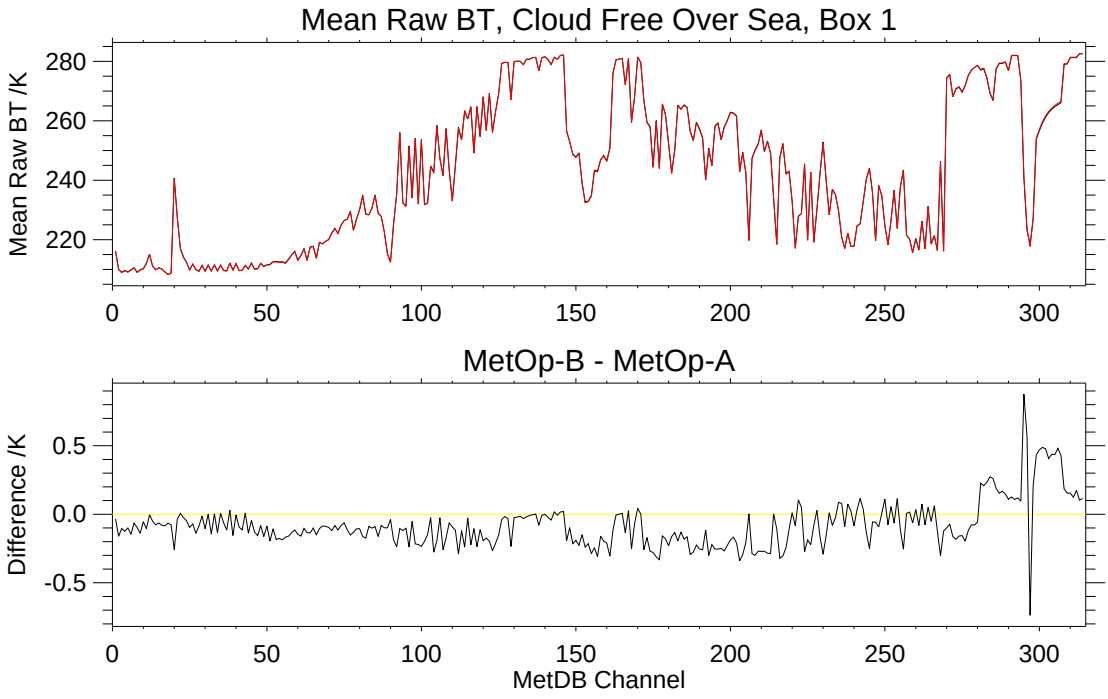

Figure 7: The same as figure 6 but for observations inside the box during period 1.

© Crown Copyright 2013

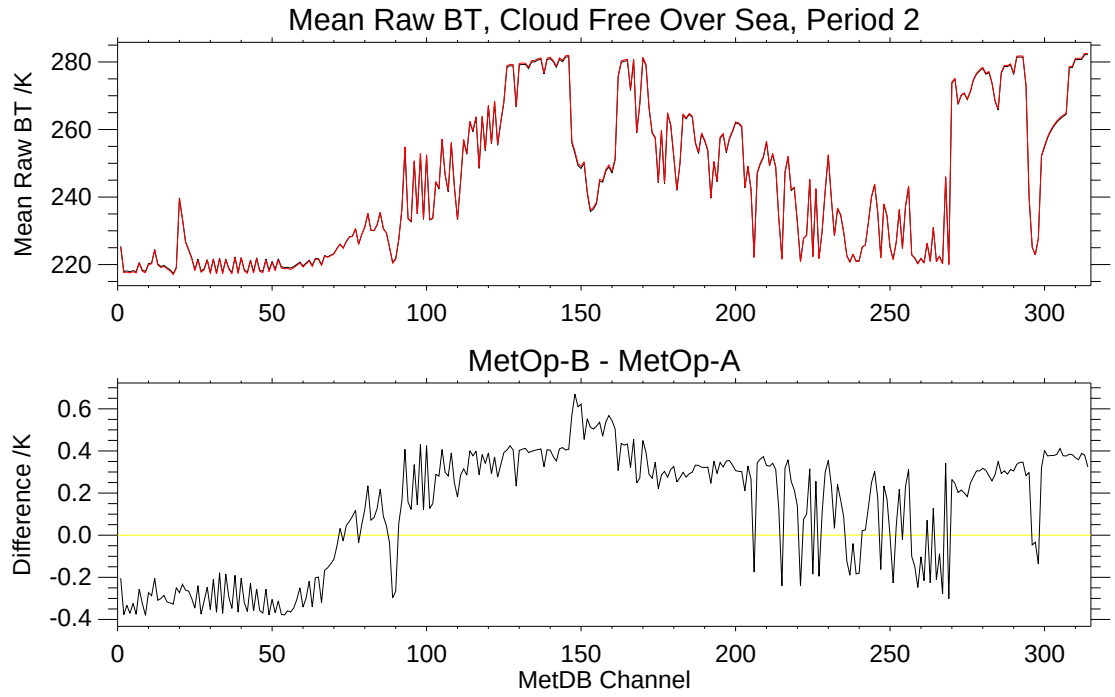

Figure 8: The same as figure 6 but for period 2. Note that the vertical scales have been adjusted.

time-period, but for observations within the box shown in figure 3 (i.e. the Box 1 data set). Here the raw brightness temperatures are in closer agreement, which suggests more even sampling. Figure 8 shows the same statistics from the second time-period (Period 2). Period 2 shows a similar skew to Period 1, although some of the short-wave channels are in better agreement.

Figure 9 is arranged in the same way as figure 6 but it shows the mean bias corrected minus forecast background (Cor-Back). There is a strong residual bias for the ozone channels (147-161). The ozone profile used at the Met Office is a scaled reference profile with the value for total column ozone being derived from monthly coefficients, using the temperature at 70 hPa as a predictor. This scheme is not particularly effective! There is also quite a lot of residual bias in the water-vapour channels. From the perspective of MetOp-B data quality, the important thing is the difference between the residual bias of MetOp-A and MetOp-B. The difference is typically less than 0.1 K. The mean bias of the the stratospheric channels (0-70) appears to be different from the rest of the channels. This difference mirrors the difference seen in raw brightness temperature (figure 6) and indicates it is probably due to differences in sampling. Channel 297 is a very high peaking short-wavelength channel and again the difference is probably because of differences in sampling. An interesting feature is the zigzagging of the difference of Cor-Back in the main long-wave CO_2 temperature sounding band – around channel 100. The brightness temperature of adjacent channels varies rapidly in this region so they are sensitive to the spectral calibration. This issue is discussed further in section 2.3.

Figure 10 shows the same statistics as figure 9 but for the ‘Box 1’ data set. The two plots

© Crown Copyright 2013

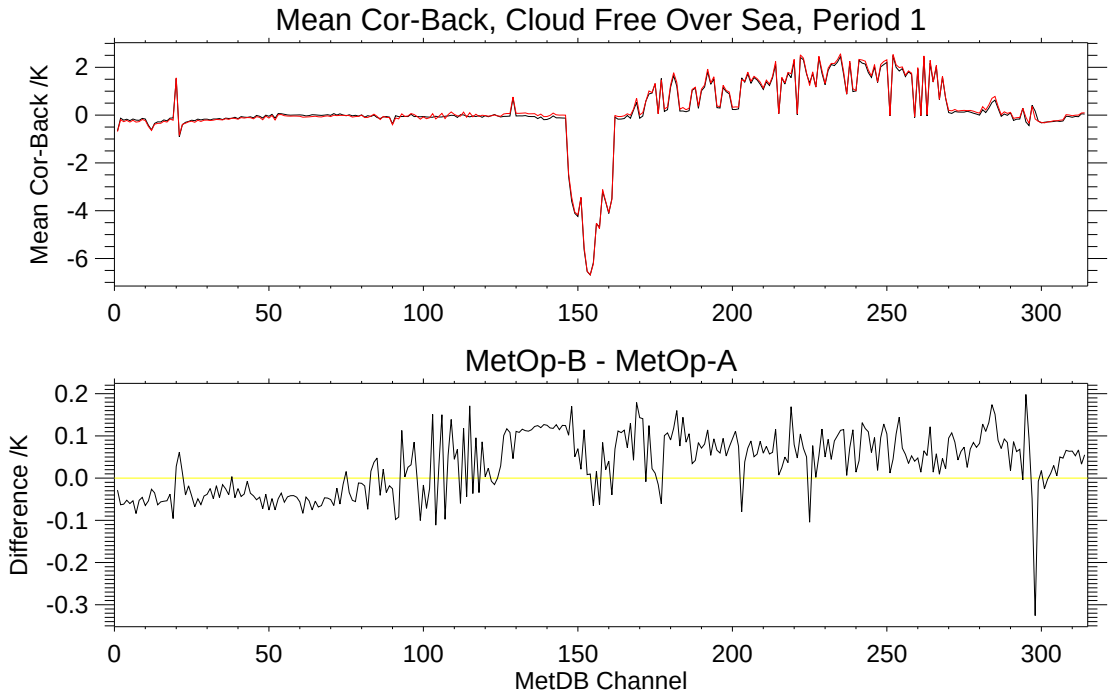

Figure 9: The mean bias corrected brightness temperature minus forecast background for cloud-free observations over the sea for IASI MetOp-A (black) and IASI MetOp-B (red). The difference is shown in the lower plot.

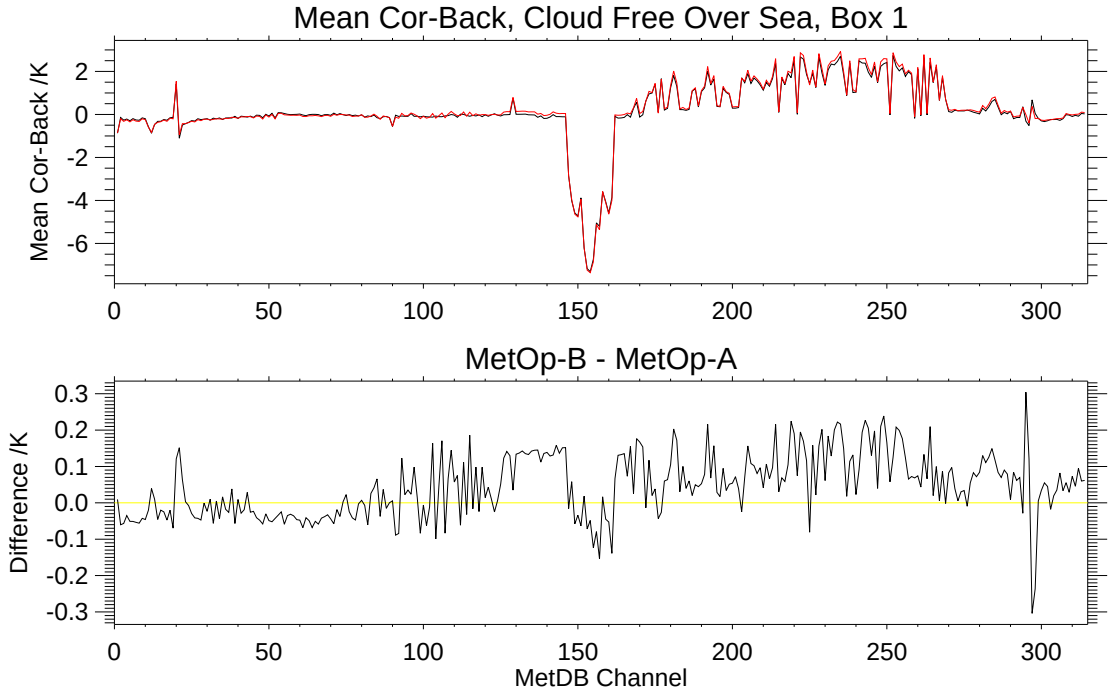

Figure 10: The same as figure 9 but for observations inside the box during period 1.

© Crown Copyright 2013

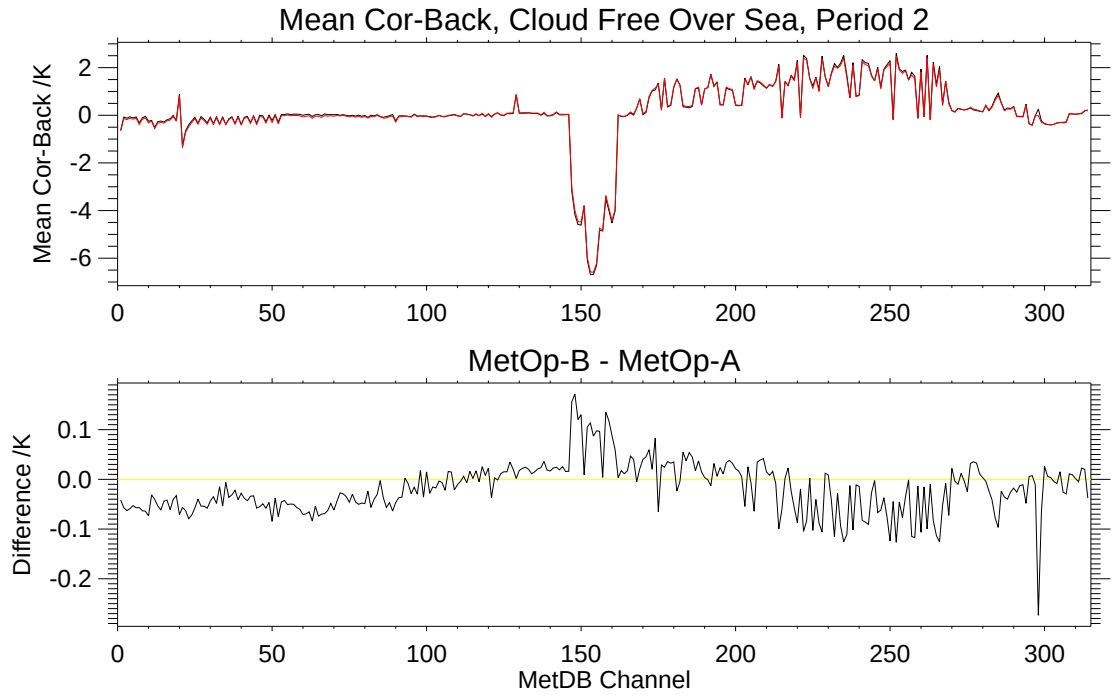

Figure 11: The same as figure 9 but for period 2.

are quite similar despite the different sampling indicated by the raw brightness temperature plots (figures 6 and 7). The analogous plot for Period 2 is shown in figure 11. The ozone channels are quite prominent in the difference plot, but it is probably a mistake to read too much into this given the large bias in ozone channels and inevitable differences in sampling. Significantly, the zigzagging in the difference of mean Cor-Back around channel 100 is no longer present.

Figures 12, 13, and 14 are similar plots to figures 9, 10, and 11, except for the standard deviation of bias corrected minus forecast background. These plots show that the standard deviation of Cor-Back is around 10% lower for the long-wavelength CO_2 channels, similar for the water vapour channels, and perhaps 5–10% lower for the short-wave channels. The standard deviation of the ozone channels are almost 10% higher in Period 2.

It is tempting to attribute the better standard deviation in the long-wavelength channels to the instrument and the worse standard deviation in the ozone channels to the vagaries of data sampling, but is that valid? Many of the long-wave channels are well modelled so a fall in the standard deviation of Cor-Back strongly indicates a drop in the instrument noise. The ozone channels by contrast are poorly modelled and the standard deviations shown are grossly larger than any reasonable value for the instrument noise so the increase is likely to be due to the modelling. There is good consistency across the 3 data sets studied, strengthening the case that the noise really is lower in the long-wave channels.

© Crown Copyright 2013

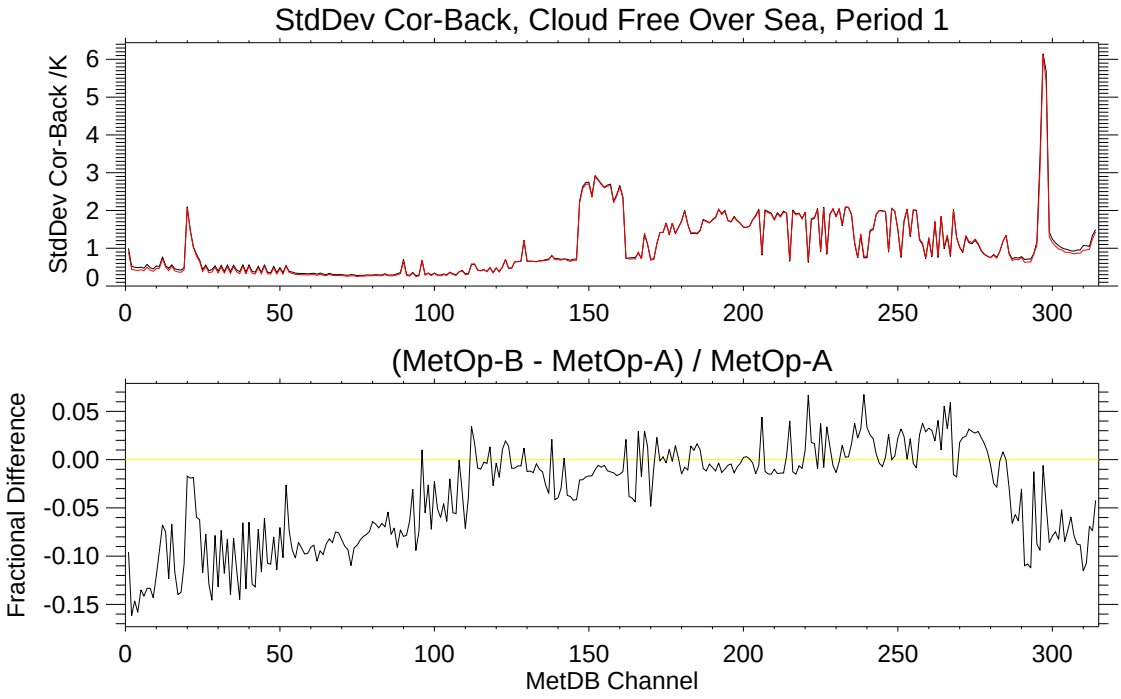

Figure 12: The standard deviation of bias corrected brightness temperature minus forecast background of cloud-free observations over the sea for IASI MetOp-A (black) and IASI MetOp-B (red). The fractional difference is shown in the lower plot.

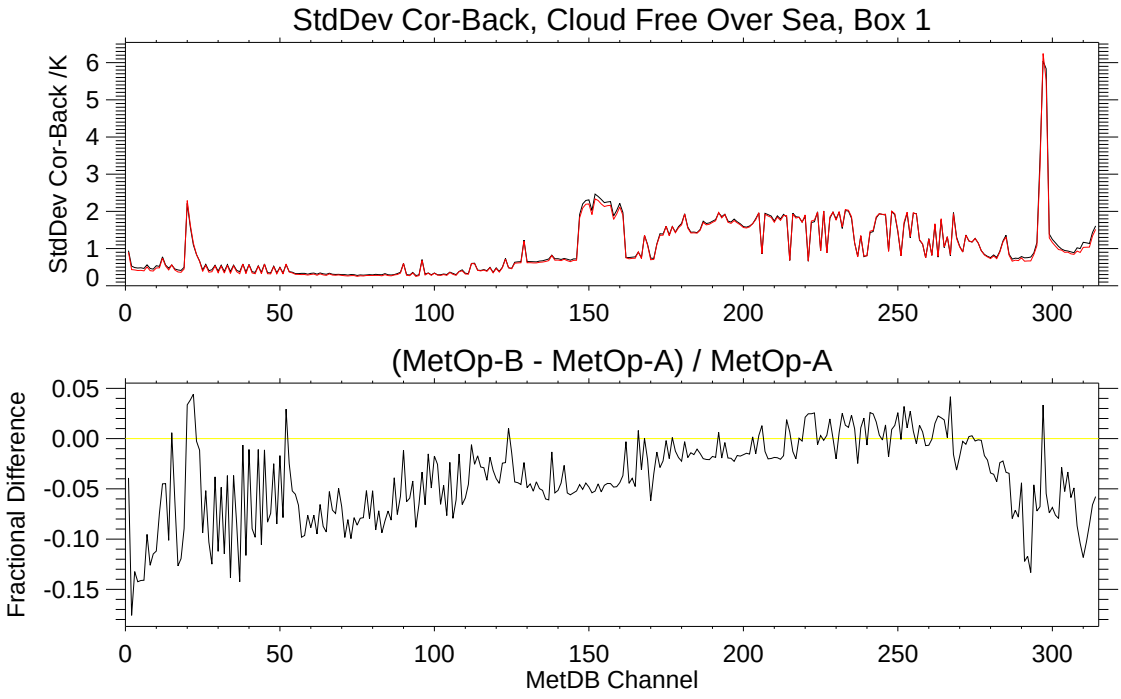

Figure 13: The same as figure 12 but for observations inside the box during period 1.

© Crown Copyright 2013

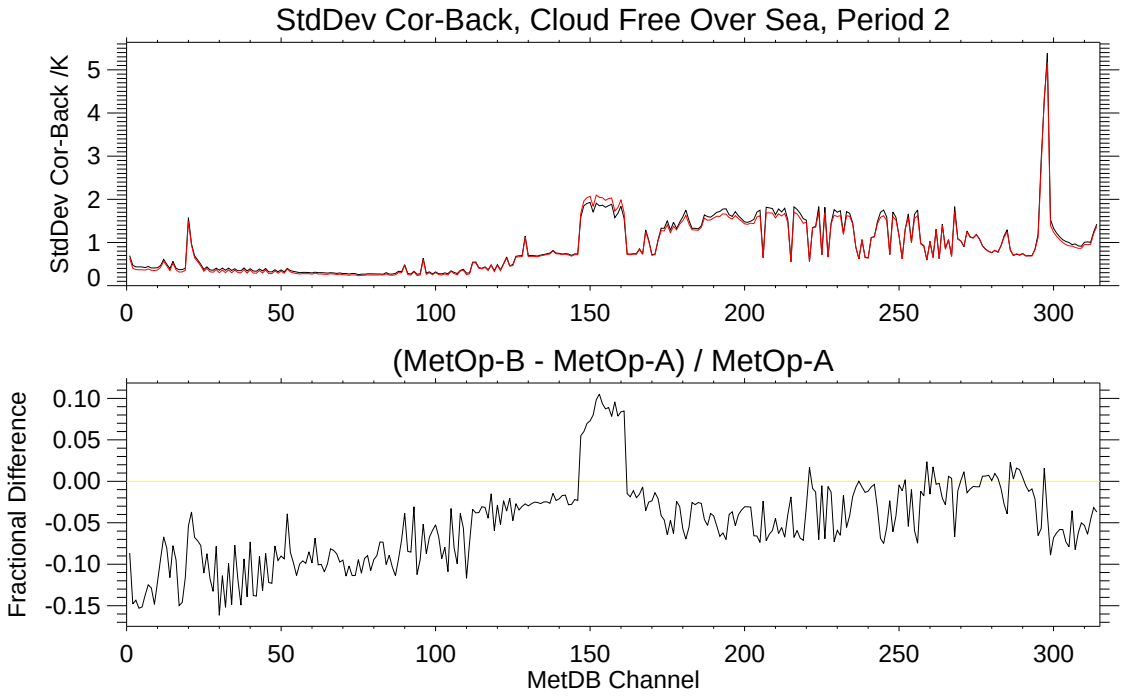

Figure 14: The same as figure 12 but for period 2.

Figure 15 shows the standard deviation of raw brightness temperature minus forecast background for Period 1. It is very similar to figure 12, showing that the bias correction is not the cause of the difference in standard deviation.

Figures 6–15 have all shown statistics derived from cloud-free observations. Figures 16–19 show means and standard deviation derived from channels that peak above the fitted cloud top. The channels shown are the ones that would be passed on to VAR for assimilation, although a few of these channels are in fact dropped at the VAR stage. These plots show the same general features as before: there is zigzagging of the difference in mean Cor-Back in Period 1, but not in Period 2; and the standard deviation of Cor-Back is around 10% lower for long-wave channels on MetOp-B.

© Crown Copyright 2013

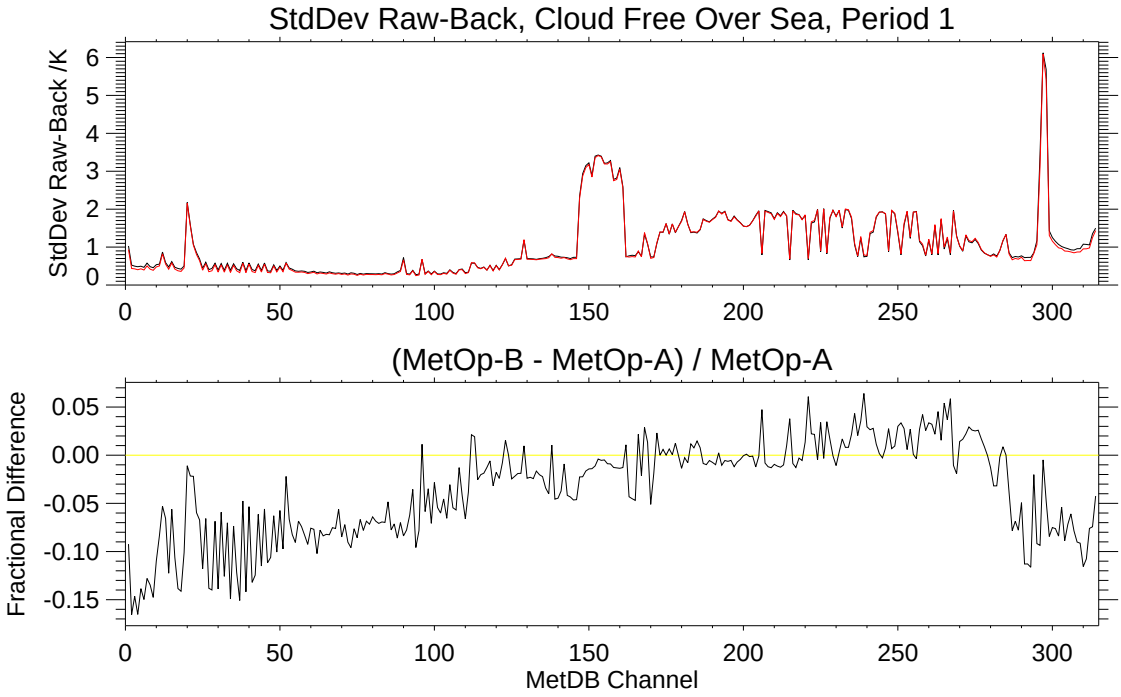

Figure 15: The same as figure 12 except for the standard deviation of *raw* brightness temperature minus background.

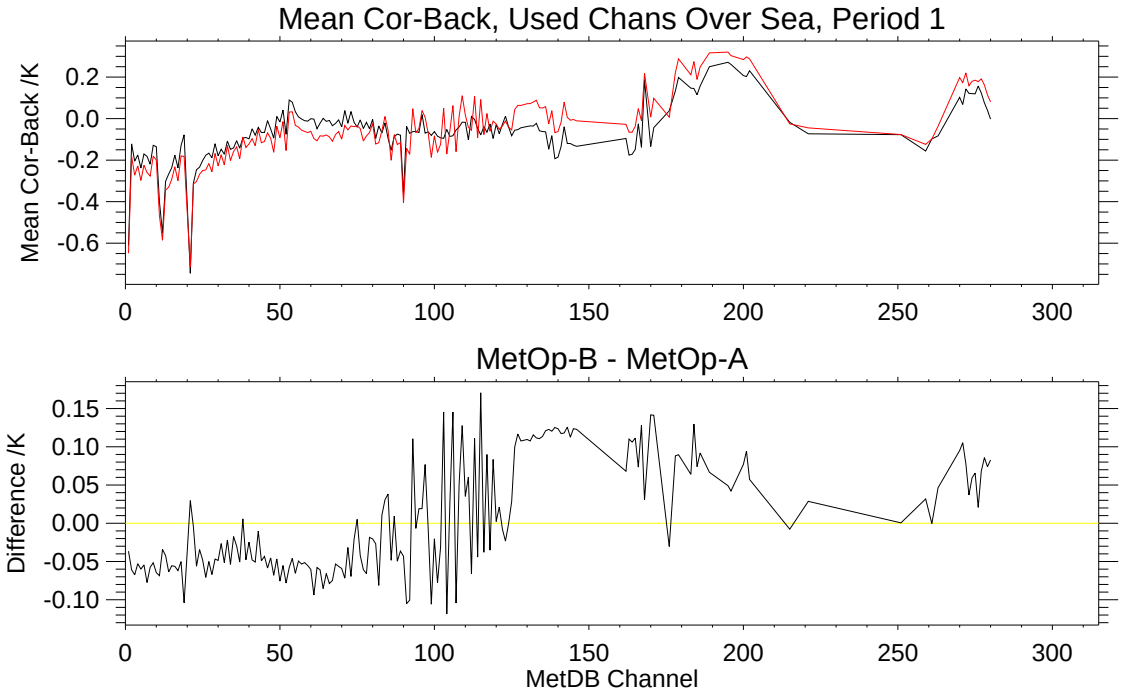

Figure 16: The mean bias corrected brightness temperature minus forecast background for channels selected for assimilation from observations over the sea for IASI MetOp-A (black) and IASI MetOp-B (red). The difference is shown in the lower plot.

© Crown Copyright 2013

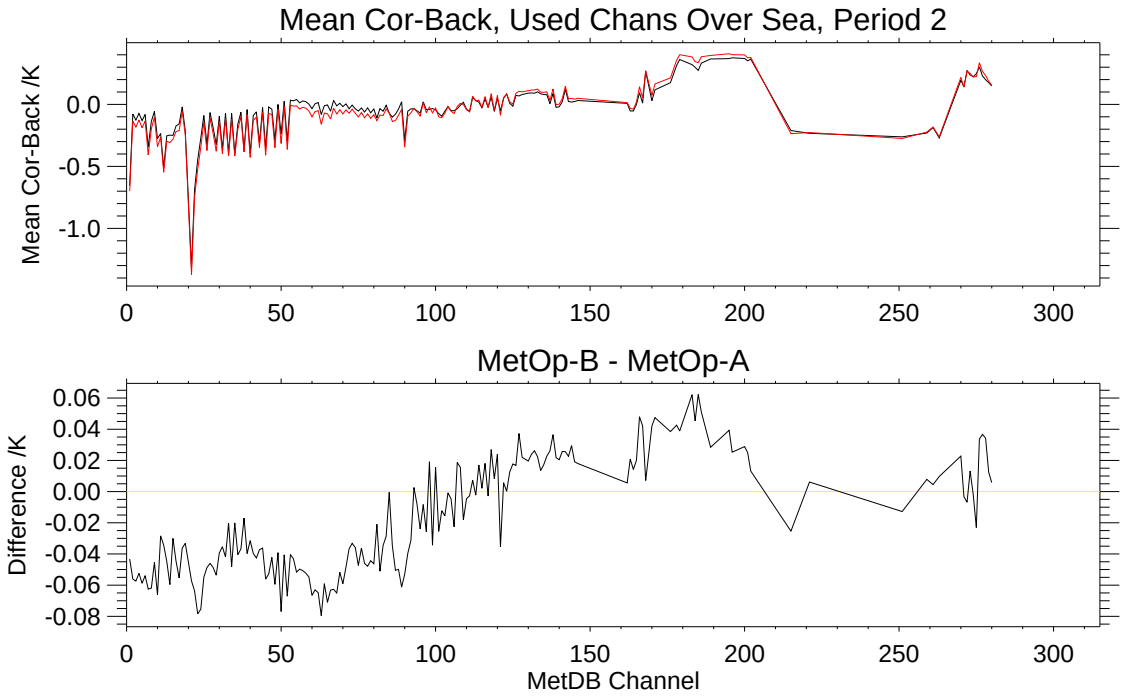

Figure 17: The same as figure 9 but for period 2.

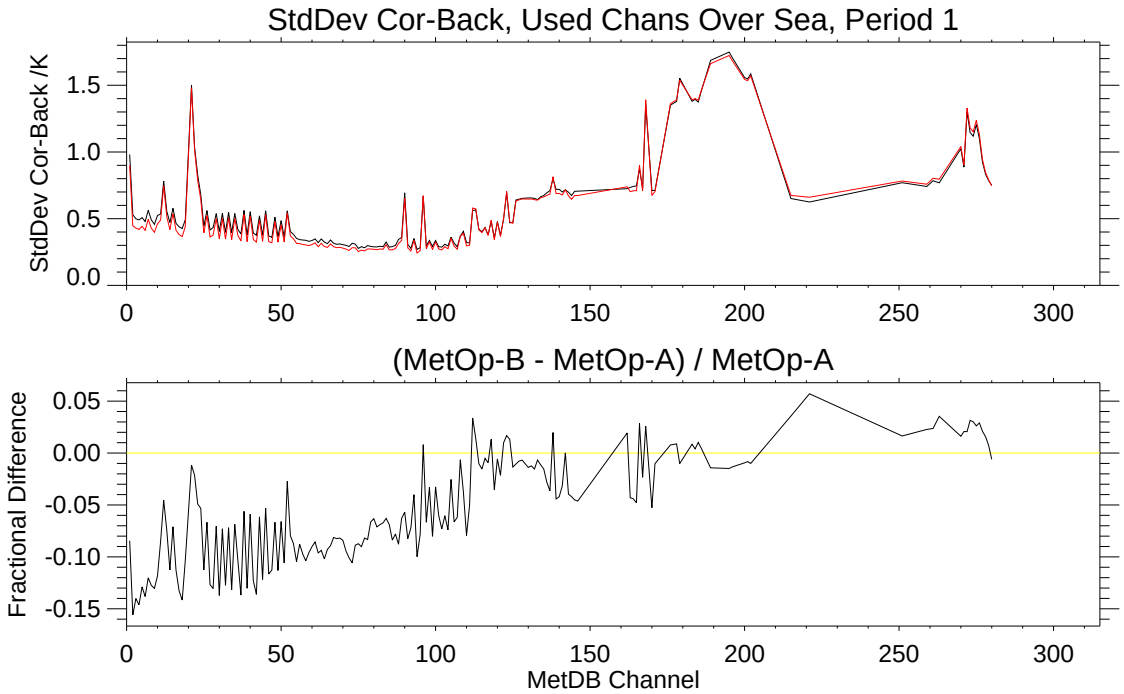

Figure 18: The standard deviation of bias corrected brightness temperature minus forecast background for channels selected for assimilation from observations over the sea for IASI MetOp-A (black) and IASI MetOp-B (red). The fractional difference is shown in the lower plot.

© Crown Copyright 2013

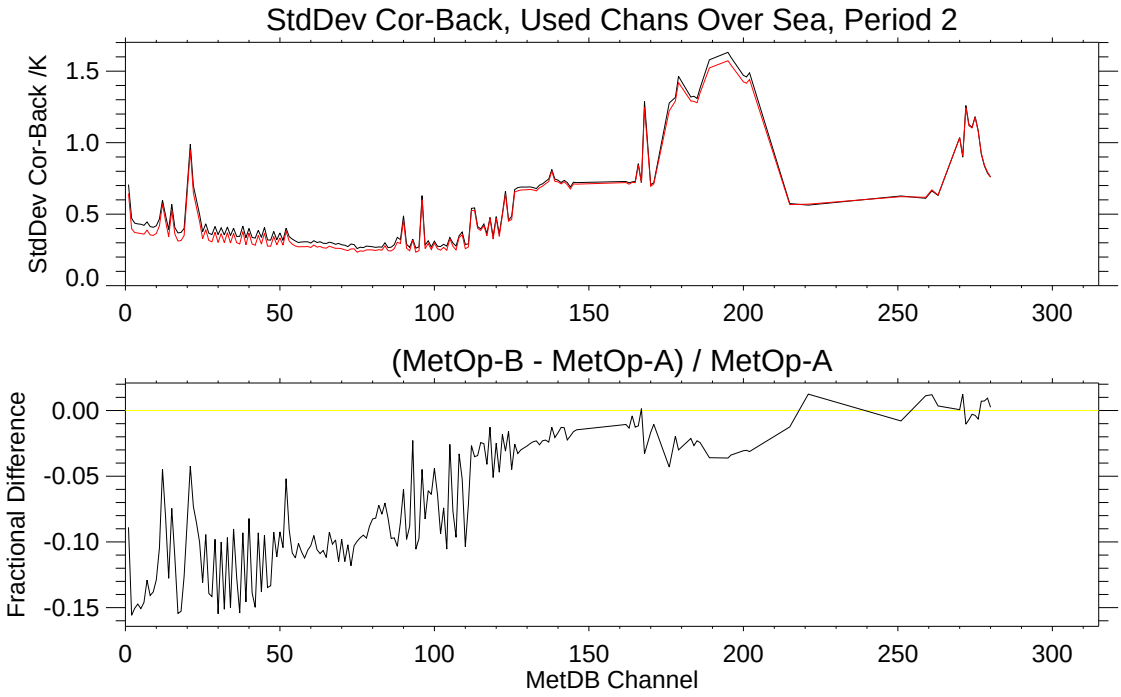

Figure 19: The same as figure 12 but for period 2.

2.3 Spectral calibration

The reduction in zigzagging of the difference in bias between MetOp-B and MetOp-A suggests that the change in spectral calibration on 10 January 2013 has brought MetOp-B into better agreement with MetOp-A. Figure 20 shows histograms of bias corrected minus background brightness temperature for 6 channels in Period 1 (note that the MetOp-B histograms have been scaled to match the number of entries in MetOp-A). There are a range of small, but very visible, positive and negative displacements of the MetOp-B distributions relative to MetOp-A. Figure 21 shows histograms for the same channels for Period 2. The distribution centres are now in very good agreement with the MetOp-B distributions being slightly narrower.

2.4 Inter-pixel differences

IASI takes measurements of 4 fields of view simultaneously. In the OPS these fields of view are called pixels and are numbered 1–4. The bias of each of these pixels could be different in principle, although in practise the differences are small for MetOp-A. The Met Office bias correction scheme currently applies the same bias correction to all pixels.

Figure 22 shows the difference between the mean Cor-Back for each pixel and the mean for all four pixels for both MetOp-A (top plot) and MetOp-B (bottom plot). The pixel biases are more tightly grouped for MetOp-B than for MetOp-A. Figure 23 shows a similar plot for the standard deviation of Cor-Back. In MetOp-B the differences are largest in those channels that have the

© Crown Copyright 2013

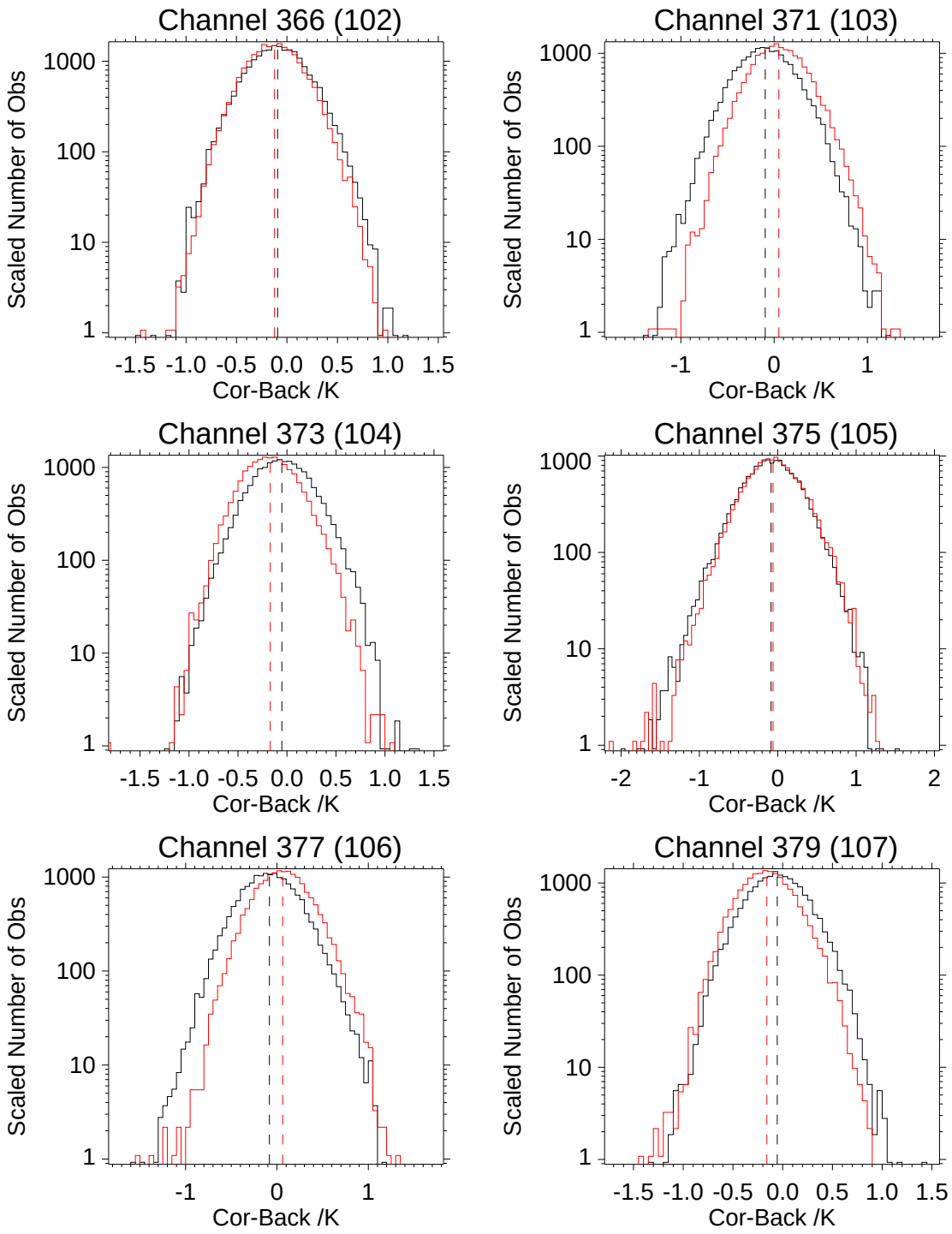

Figure 20: Histograms of bias correction minus background brightness temperature for 6 mid-tropospheric temperature sounding channels using data from period 1.

© Crown Copyright 2013

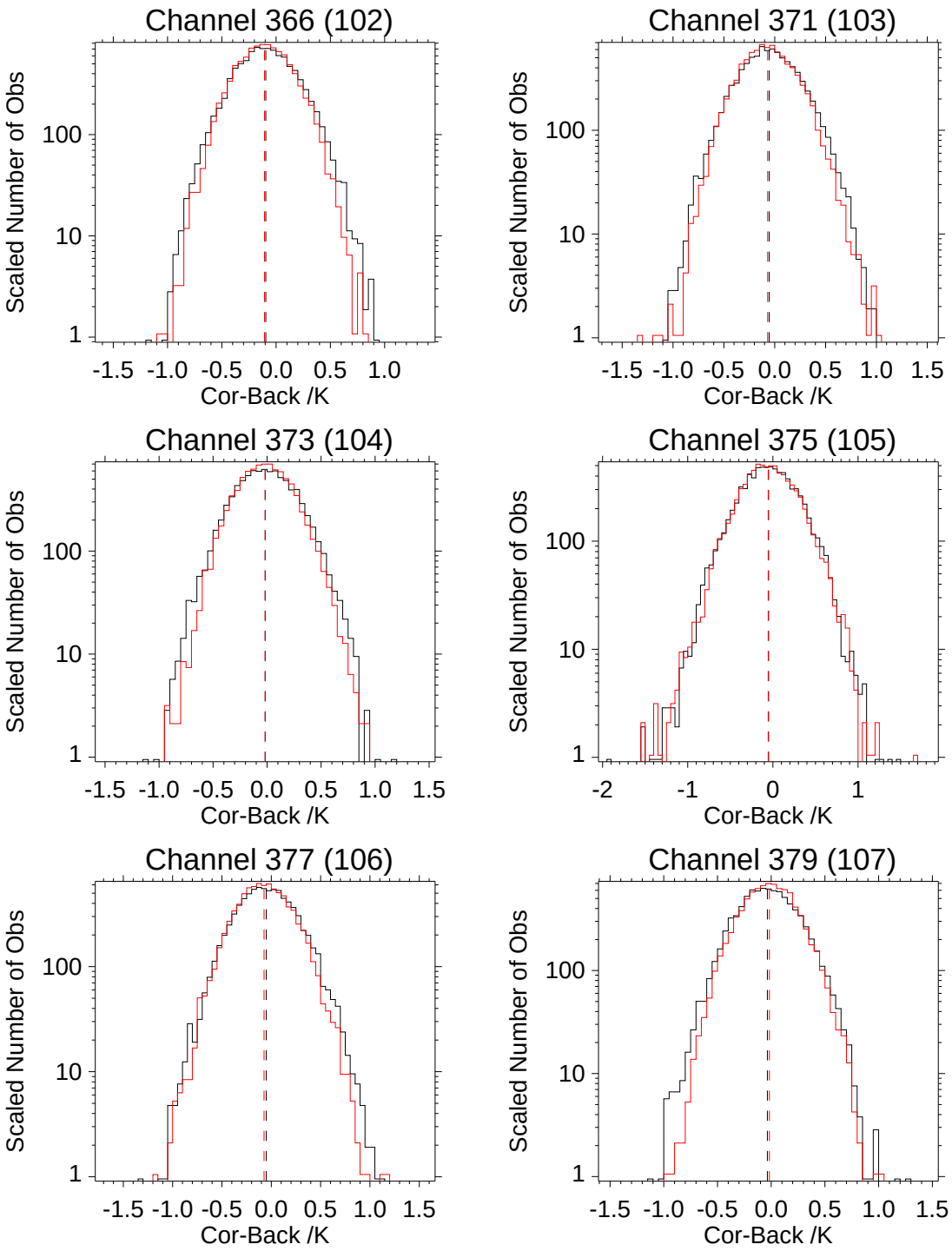

Figure 21: The same as figure 20 but using data from period 2.

© Crown Copyright 2013

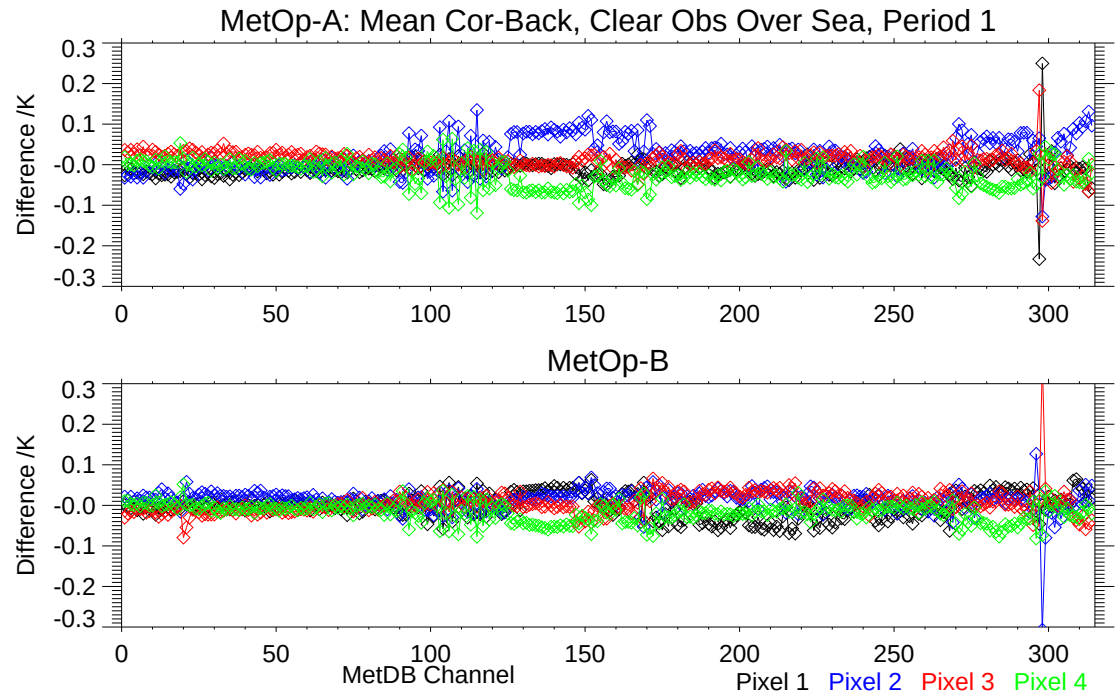

Figure 22: The difference between the mean Cor-Back of each pixel and the mean Cor-Back of all four pixels. MetOp-A is shown in the upper plot and MetOp-B below.

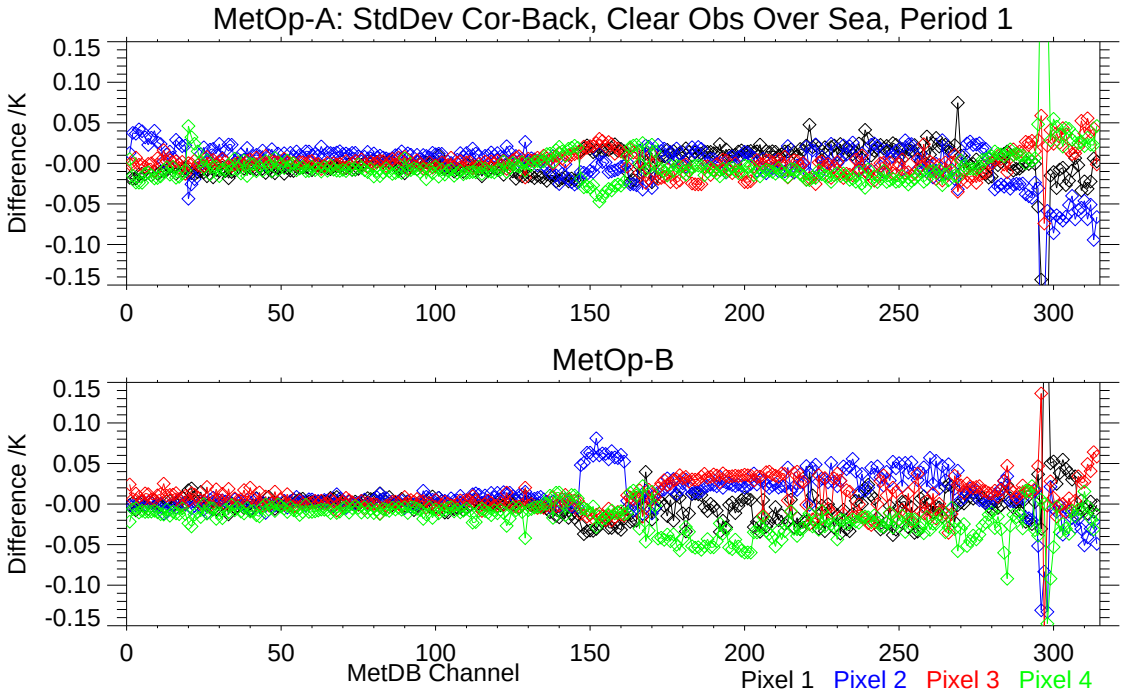

Figure 23: The difference between the standard deviation of Cor-Back of each pixel and the standard deviation of Cor-Back including all four pixels. MetOp-A is shown in the upper plot and MetOp-B below. 2 or 3 of the high-peaking short-wave channels extend to beyond the scale shown but none go beyond ±0.5K.

© Crown Copyright 2013

largest standard deviations (ozone, water vapour, and a few high-peaking short wave channels). Overall the performance of the 4 pixels appears to be at least as well matched on MetOp-B as they are on MetOp-A.

3 Conclusions

The fit of locally received MetOp-B IASI observations to the forecast background has been compared to that of MetOp-A observations in the vicinity of Exeter. The bias of MetOp-B IASI channels appears to be same as MetOp-A within 0.1 K, and some of the differences are likely to be result of differences in sampling. The standard deviation of bias corrected minus forecast background is around 10% less for MetOp-B than for MetOp-A for the long-wavelength and short-wavelength channels, indicating a lower instrument noise in those channels. The spectral calibration of MetOp-B moved closer to that of MetOp-A on the 10 January 2013. Inter-pixel biases are smaller in MetOp-B IASI than in MetOp-A IASI. From the evidence in this study, the quality of MetOp-B data appears to be at least as good as MetOp-A with slightly lower noise.

© Crown Copyright 2013

Met Office
FitzRoy Road, Exeter
Devon, EX1 3PB
UK

Tel: 0870 900 0100
Fax: 0870 900 5050
enquiries@metoffice.gov.uk
www.metoffice.gov.uk

Produced with the Met Office LaTeX template v2.0.0